Visible-Light-Degradable 3D Microstructures in Aqueous Environments

Marvin Gernhardt, Vinh X. Truong,* and Christopher Barner-Kowollik*

The additive manufacturing technique direct laser writing (DLW), also known as two-photon laser lithography, is becoming increasingly established as a technique capable of fabricating functional 3D microstructures. Recently, there has been an increasing effort to impart microstructures fabricated using DLW with advanced functionalities by introducing responsive chemical entities into the underpinning photoresists. Herein, a novel photoresist based on the photochemistry of the bimane group is introduced that can be degraded upon exposure to very mild conditions, requiring only water and visible light (λ_{max} = 415–435 nm) irradiation. The degradation of the microstructures is tracked and quantified using AFM measurements of their height. The influence of the writing parameters as well as the degradation conditions is investigated, unambiguously evidencing effective visible light degradation in aqueous environments. Finally, the utility of the photodegradable resist system is demonstrated by incorporating it into multimaterial 3D microstructures, serving as a model for future applications.

1. Introduction

Direct laser writing is a well-established additive manufacturing technique based on two-photon polymerization, extensively used for the fabrication of 3D micro- and nanostructures.[1] In DLW, a pulsed femtosecond laser is employed to generate a diffraction-limited voxel—the 3D analogue to a pixel—within a viscous photoresist. The polymerization is initiated by two-photon absorption which, due to the super-linear effect, enables the exposed volume to be restricted to the small-scale voxel space.[2] 3D scanning of the voxel subsequently generates microstructures of (near) arbitrary shape. Such complex and highly resolved structures have been used in a plethora of functional devices for applications ranging from microelectronics[3] to microfluidic devices,[4] to microscaffolds for cell cultures and bioengineering.[5,6]

The application of microstructures fabricated by DLW in functional devices requires a variety of materials with different electrical, optical, mechanical and chemical properties. Materials that are adaptive, i.e., their properties can be tailored post-fabrication, are highly desirable, with degradability being one of the most sought-after adaptive properties.[7–9] However, the crosslinked polymer structures generated during DLW—especially when using commercial photoresists—are permanent. Degrading such materials often requires harsh conditions, e.g., high temperature hydrolysis of the ester bonds in the classic (meth) acrylic networks or laser ablation.[7,8] Various chemical functionalities have been incorporated into the photoresist formulation to enable rupture of the printed structure under specific stimuli such as chemical agents,[10–12] enzymes,[13] temperature, or light.[14] Among those, light is the trigger of choice to provide spatial and temporal control over the degradation process.

To introduce photodegradability into microstructures, a photolabile moiety has to be integrated into the photoresist's chemical structure. A critical challenge in designing photodegradable DLW resists is to select a suitable photolabile group that is stable during the writing process. Certain photochemical reactions such as the reversible photodimerization of chemical entities including coumarins, anthracene and cinnamate may be suitable for these purposes since their dimerization/crosslinking can be induced by UV light at 300 to 400 nm, and the cycloelimination can occur under irradiation of shorter wavelength UV light (≤260 nm).[15] However, such high energy UVA/UVB irradiation can be too severe for many applications, specifically cell scaffolding. Possibly more suitable visible-light-responsive photolabile moieties, however, degrade rapidly under UV light, and thus cannot survive the writing process, which mostly employs such UV wavelengths.[16] So far, there is only one report by our team on photodegradable networks obtained from DLW, in which both the writing and

M. Gernhardt, V. X. Truong, C. Barner-Kowollik
School of Chemistry and Physics
Queensland University of Technology (QUT)
2 George Street, Brisbane, QLD 4000, Australia
E-mail: truongvx@qut.edu.au; christopher.barnerkowollik@qut.edu.au
M. Gernhardt, V. X. Truong, C. Barner-Kowollik
Centre for Materials Science
Queensland University of Technology (QUT)
2 George Street, Brisbane, QLD 4000, Australia
C. Barner-Kowollik
Institute of Nanotechnology
Hermann-von-Helmholtz-Platz 1
Karlsruhe Institute of Technology (KIT)
76344 Eggenstein-Leopoldshafen, Germany

ADVANCED
SCIENCE NEWS
www.advancedsciencenews.com
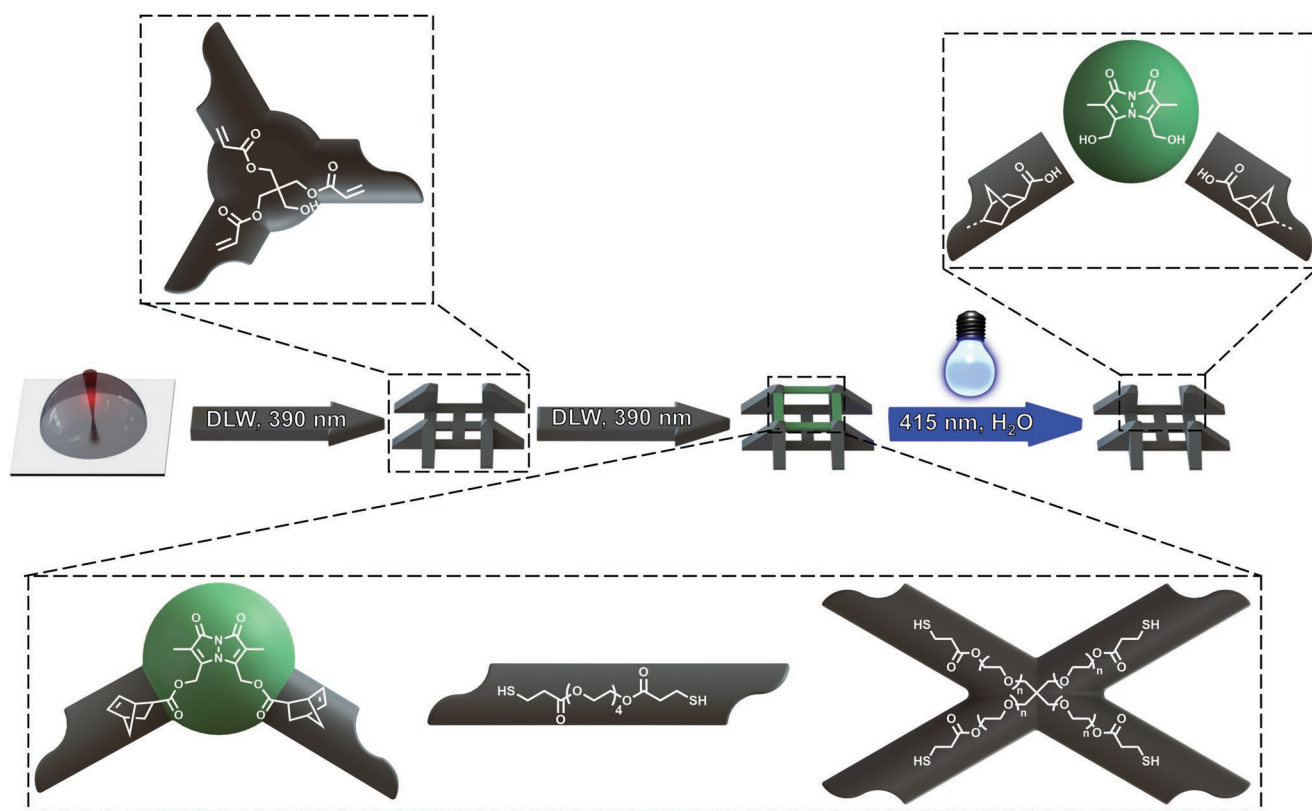
ADVANCED
MATERIALS
www.advmat.de

Figure 1. Concept for visible-light-degradable 3D printed multimaterial microstructures in aqueous environments: In the initial DLW step, static frames are fabricated from a commercial resist. In the subsequent step, bridges are fabricated within these frames from our degradable resist formulation, consisting of a bimane norbornene linker, TEG-SH, and a 4-arm PEG-SH. These bridges can subsequently be degraded under irradiation with visible light in aqueous environments, where the bimane ester function is cleaved.

erasing processes employs relatively mild irradiation conditions.[14] Specifically, we prepared a difunctional acrylate crosslinker containing a photolabile *o*-nitrobenzyl ether moiety, which was crosslinked using a visible light initiator (Ivocerin, λ_{max} = 408 nm), and subsequently degraded by UV light (λ_{max} = 365 nm). To date, a photoresist formulation that permits visible light erasure of the DLW structure post-fabrication still remains elusive, including in aqueous environments.

Herein, we introduce a DLW resist that allows photocrosslinking by UV light (λ_{max} = 380–390 nm), or the near-infrared 780 nm employed in the two-photon absorption-based DLW, and photodegradation with visible light (λ_{max} = 415–435 nm). Our approach utilizes the thiol–norbornene photo-click reaction for rapid photopolymerization, and photodegradation of a bimane ester moiety for visible light (λ_{max} = 415–435 nm) induced degradation (**Figure 1**). In contrast to methacrylates, the norbornene group reacts selectively with the thiol group via step-growth polymerization, generating highly defined and homogenous structures,[17] while the bimane ester function photodegrades selectively in the presence of protic solvents such as water and alcohol.[18–20] Critically, the choice of the thiol–ene reaction ensures the incorporation of a photocleavable group for every crosslink formed, ensuring that complete degradation can occur in the resultant network. The herein pioneered photoresists can thus be orthogonally crosslinked by long wavelength UV light and degraded by

redshifted visible light—a feat that has not been previously realised in 3D printed structures.

2. Results and Discussion

Both components of our resist can be readily prepared from commercially available materials via one-step procedures in high yields (**Figure 2**A). Specifically, the 4-armed or linear PEG-SH was prepared by Fischer esterification of a 4-arm or linear PEG-OH on the gram-scale with yields in the range of 85–90%, whereas the bimane-Nb was prepared from bimane dibromide and norbonene carboxylic acid by Finkelstein esterification with a yield of 87% (refer to the Supporting Information for the full synthetic procedures). The introduced functionalities enable two distinct photochemical transformations: photocrosslinking of the thiol and norbornene functions under irradiation with UV light (λ_{max} = 380 nm) and photocleavage of the bimane ester under irradiation with visible light (λ_{max} = 420 nm) (Figure 2B).

Initially, we investigated the photocrosslinking and photodegradation of the resist by rheological measurements, The sequence of the rheology measurements is shown in Figure 2C. First, a mixture of 4-arm PEG-SH and bimane dinorbornene (1:1 molar ratio, in acetonitrile c = 5 M) was irradiated with UV light (λ_{max} = 380 nm). The sharp increase in
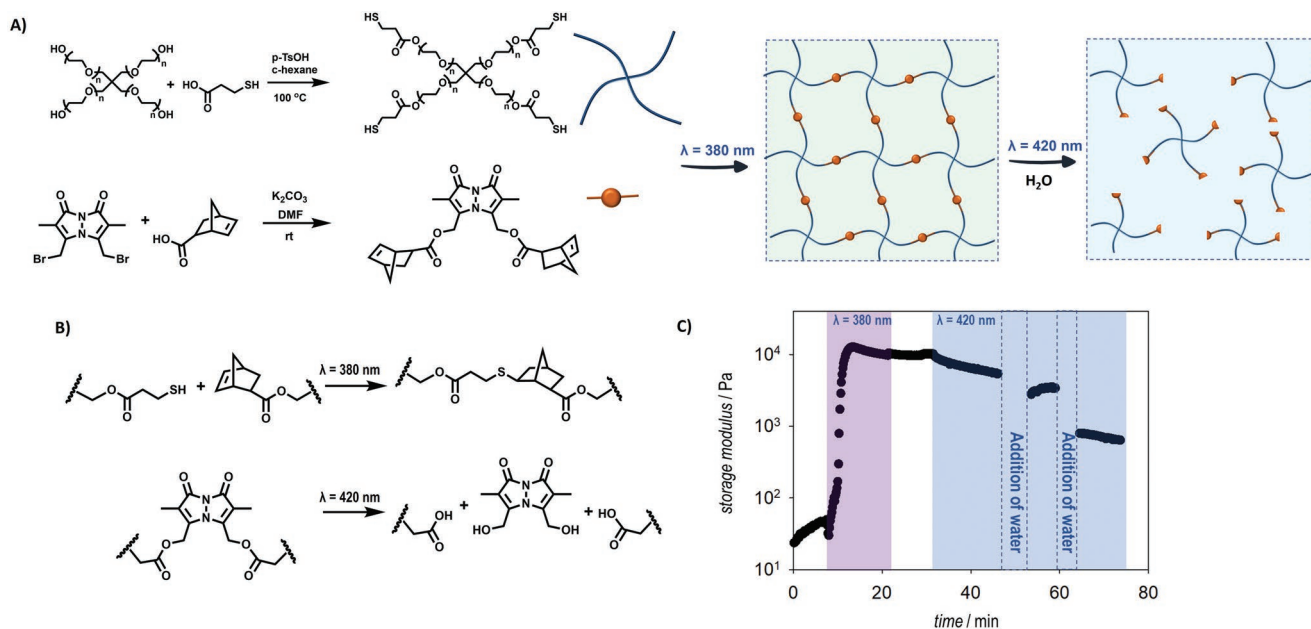
Figure 2. A) Synthesis of 4-armed PEG-SH and bimane di-norbornene as the major components of the photodegradable resist and schematic photocrosslinking and photodegradation of the network. B) Mechanism of photocrosslinking by UV light (380 nm) and photodegradation by blue light (420 nm). C) Rheological assessment of the photocrosslinking and photodegradation. The sample was first crosslinked under irradiation with 380 nm. The irradiation wavelength was switched to 420 nm, leading to degradation. Water was added to the sample while being subjected to irradiation in two steps during which data could not be recorded (dashed lines), leading to a significant decrease in the storage modulus.

the storage modulus (G') indicates rapid crosslinking, with complete gelation observed after 2 min. Further irradiation on the mixture resulted in a slight decrease of the G' value, which may be attributed to the moisture presented in acetonitrile and ambient air, since a protic solvent is required for the photolysis of bimane (Scheme S1, Supporting Information).[18] In the subsequent step, the formed gel was irradiated with blue light (λ_{max} = 420 nm), leading to a further decrease in G'. Addition of water, during which the measuring plate was removed from the rheometer and the acquisition of data was paused, resulted in a more rapid decrease in G'. Over the course of 1 h of irradiation, the G' value decreased by one order of magnitude from ca. 10 000 Pa to ca. 1000 Pa, indicating successful degradation of the crosslinked structure. We further examined the effect of solvent on the photolysis by undertaking additional rheological experiment in which a solvent mixture was added without disturbing the rheology set-up. Immersing the crosslinked material in a solvent mixture of water/acetonitrile (v/v = 2/8) enabled effective degradation under blue light irradiation (Figure S3, Supporting Information), whereas very slow degradation was observed when the material was not in contact with water (Figure S4, Supporting Information).

Having confirmed the efficient photocrosslinking and photodegradation profiles, we subsequently applied our new resist system during DLW. When formulating the resist composition, we added an additional bifunctional thiol linker based on tetraethylene glycol (TEG)—prepared in the same way as the 4-arm linker—to the mixture to enhance the degradation of the network post-fabrication. Here, linear TEG-SH was used as a co-solvent and to reduce the crosslinking density of the network, facilitating water diffusion, enabling efficient photodegradation. Without the addition of TEG-SH, we did

not observe significant degradation after 30 h of irradiation (Figure S11, Supporting Information). The necessity to add bifunctional crosslinker to reduce the crosslinking density for efficient photodegradation of the microstructures has been observed previously in the literature.[21] A molar ratio of 1:1:2 between the 4-arm PEG-SH, the bifunctional TEG-SH and the bimane di-norbornene crosslinker was thus selected as the optimal composition that was used for all microstructures discussed herein. This ratio enables both the formation of microstructures with good structural integrity and efficient degradation. A higher molar ratio of TEG-SH to 4-arm PEG-SH resulted in unstable microstructures (Figure S12, Supporting Information). The final resist formulation also contained propylene carbonate to dissolve the bimane crosslinker and 1% mol Irgacure 369 as a photoinitiator.

With the optimal resist formulation at hand, we next fabricate arrays of conical microstructures (Figure S13, Supporting Information). The arrays consist of microstructures written using different printing parameters. The model used to fabricate the cones has a base diameter of 20 µm and a height of 5 µm (Figure S14, Supporting Information). In DLW, the two most important writing parameters are the laser power and the scan speed.[22] Together, they effectively determine how long a certain voxel is exposed to a certain amount of laser intensity. Here, the laser power was varied between 6 and 14 mW and the scan speed was varied between 200 and 10 000 µm s^{-1}. If the laser exposure is too high, microexplosions can occur, leading to distorted structures. If the laser exposure is too low, no microstructures are fabricated at all, as the threshold for initiation is not reached. It is well documented in the literature that these writing parameters affect the mechanical properties of the fabricated microstructures,[23] as well as the resolution
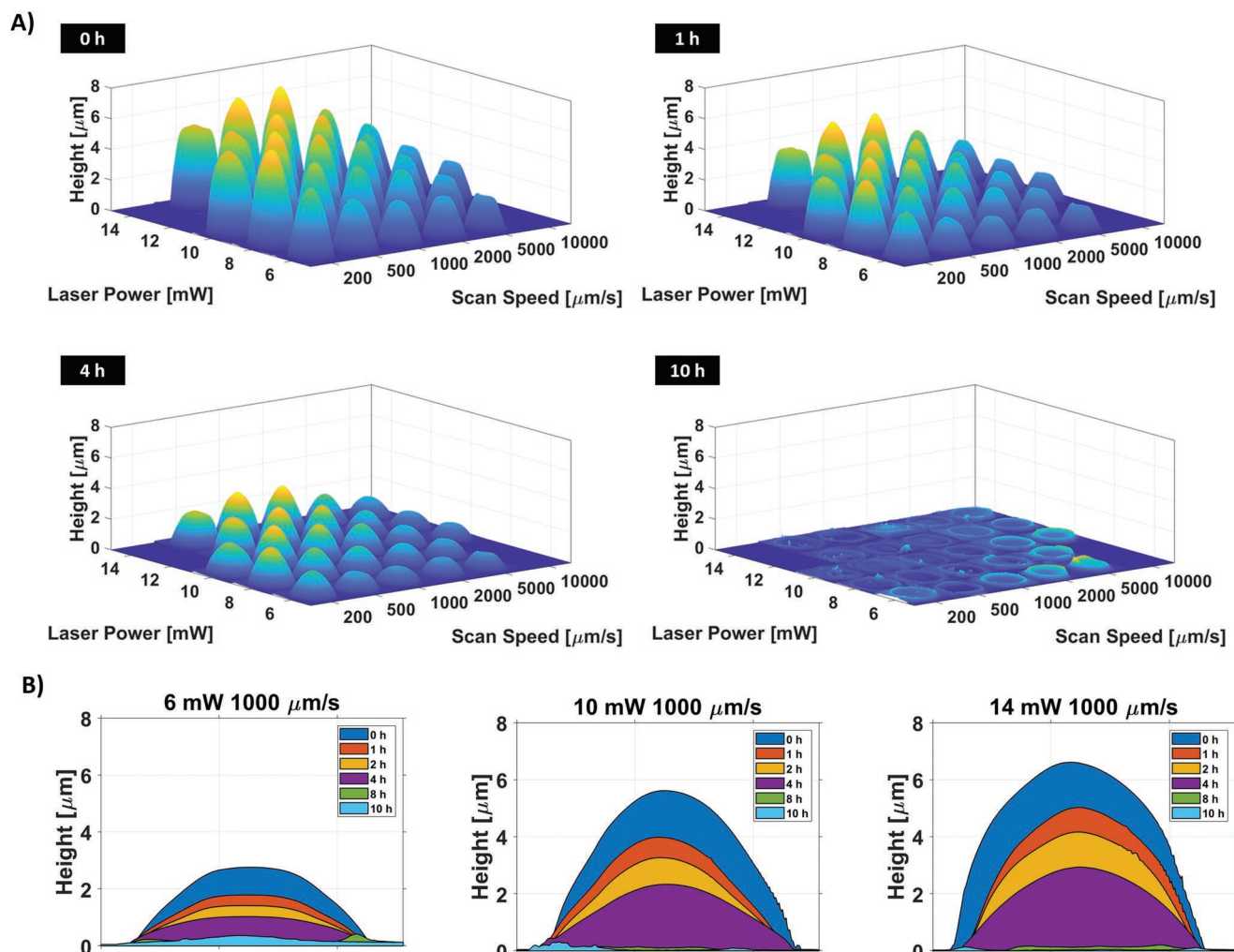
Figure 3. Degradation of conical microstructures upon λ_{max} = 415 nm irradiation in water. A) AFM height data for microstructure arrays fabricated using different laser powers and scan speeds after several degradation steps. B) AFM height data of the contours at the maximum height of selected microstructures fabricated with different laser powers, but identical scan speed over the course of degradation for 10 h, negligible material heights were detected at 8 h (green) and 10 h (light blue).

of individual features, as the laser power influences the size of the voxel.[24] As the solid, polymerized phase has a higher density than the liquid resin due to covalent bonds being formed, microstructures shrink during the writing process. Evaporation of the solvent used for washing during development causes capillary forces exacerbating the process.[25–27] The degree of shrinkage is also influenced by the writing parameters, therefore microstructures with various sizes were observed at different laser powers and scan speeds.

We employed atomic force microscopy (AFM), which enables accurate measurement of surface parameters,[28] to accurately follow the degradation of the microstructures over the course of irradiation in an aqueous environment. The conical shape of the microstructures was selected because of its compatibility with the AFM technique. The sloped edges without any sharp transition from the substrate make it easy for the tip to trace the entire structure while moving rapidly. The microstructure array was irradiated in several steps with a 10 W λ_{max} = 415 nm LED, while submersed in MilliQ water without any further

additives. Before irradiation and after each subsequent irradiation step, all microstructures were individually assessed via AFM, determining their height and overall shape. The AFM data was subsequently combined into the 3D arrays depicted in **Figure 3**A, displaying four representative recorded steps of the degradation in water. The entire sequence has been animated into Movie S1 and images of the remaining steps can be further found in the (Figure S15, Supporting Information). In all these figures the aspect ratio has been adjusted to make the change easier to follow. Our data displays complete degradation of the microstructures over the course of irradiation in water until only a faint outline remains. The degradation was also followed using light microscopy (Figure S16, Supporting Information); however this technique only offers a top-down view, which alone is insufficient to follow the degradation process. Figure 3B, further depicts a side view of the contours at the maximum height of microstructures written with three different laser powers.

Having printed an array of microstructures using different writing parameters allowed us to investigate the influence
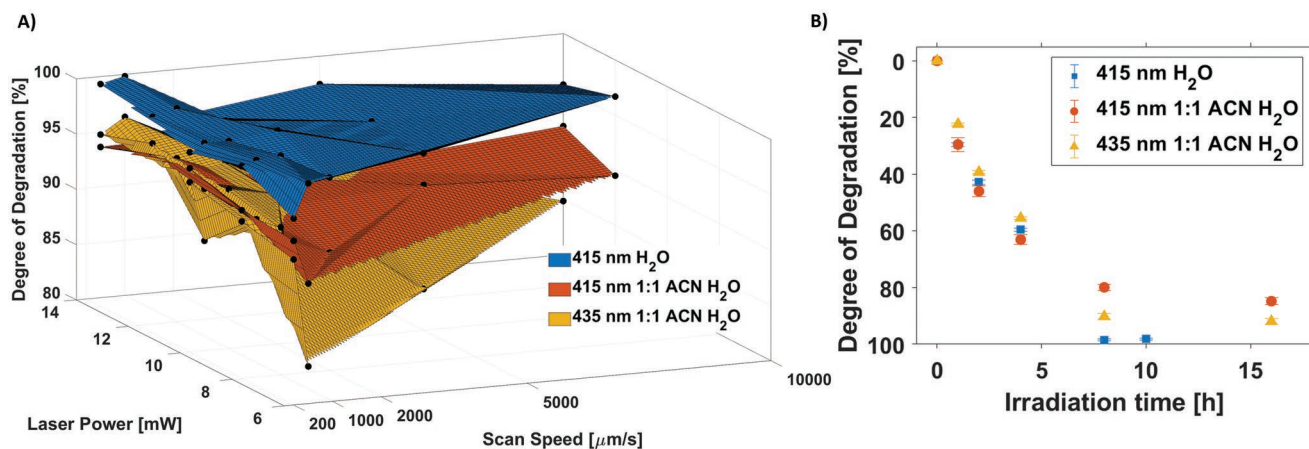
2203474 (4 of 7)

Figure 4. Degree of degradation reached over the course of degradation for microstructures fabricated using a spectrum of writing parameters under three different degradation conditions as determined by AFM. Conical microstructure samples were immersed in either pure MilliQ water or a 1:1 mixture of water and acetonitrile and irradiated with a 10 W LED (λ_{max} = 415 or 435). Only writing parameters that led to successful fabrication on all three samples are shown. A) Degree of degradation reached at the end of the of the observed degradation time for all individual microstructures fabricated using different writing parameters. B) Degree of degradation averaged over all microstructures at each point over the course of degradation.

of those parameters on the degradation. The blue surface in **Figure 4** displays a 3D plot of the degradation percentage of the same conical microstructures seen in Figure 3 as a function of laser power and scan peed, after 10 h of irradiation at λ_{max} = 415 nm in water. Here, the degree of degradation was determined from the ratio of the height of the microstructures at their centre before and after degradation. The observed general trend discernible from Figure 4 is that microstructures fabricated with higher laser powers and lower scan speeds—those that were exposed to a higher laser intensity during fabrication—degrade to a slightly higher extent than those fabricated using lower laser powers and higher scan speeds. This is surprising, as one might expect the higher degree of crosslinking induced by higher laser powers and lower scan speeds to lead to slower degradation. The observed trend might potentially be due to the more rapid crosslinking leading to a less homogeneous network with more pronounced phase separation and more dangling chain ends as the rapidly expanding network traps unreacted functionalities.[29]

We were subsequently interested in investigating different degradation conditions. Initially, we changed the solvent system from pure MilliQ water to a 1:1 mixture of water and acetonitrile (orange in Figure 4). While water or another protic solvent is necessary to induce the cleavage of the bimane group, we hypothesised that the bimane degradation products might be more soluble in acetonitrile. By dissolving those degradation products more readily, the addition of acetonitrile might thus enhance the degradation rate. Acetonitrile might also lead to increased swelling of the microstructures, further facilitating water diffusion and degradation: as the network swells, it becomes more accessible to water, enabling hydrolysis. The addition of acetonitrile did, however, not appear to enhance the degradation rate. In fact, the degradation in water proceeded to a more complete degree for microstructures fabricated using all the different writing parameters considered here compared to the other two samples. Additionally, we used a 10 W λ_{max} = 435 nm LED instead of a 10 W λ_{max} = 415 nm

LED in order assess whether the degradation would still proceed at this higher wavelength (yellow in Figure 4). Interestingly, the irradiation with λ_{max} = 435 nm still proceeds with similar efficiency as the irradiation with λ_{max} = 415 nm in 1:1 water/acetonitrile. It is notable that the degradation proceeds to at least 80% completion in all cases and to essentially 100% at slow scan speeds and high laser powers, especially in water. We submit that photodegradation in complete aqueous environment is highly useful for applications in, e.g., drug delivery and cell culture scaffolding.

We further examined the degradation of the microstructures under illumination with regular fluorescent white light lamps (refer to Figure S2, Supporting Information for the emission spectrum). Over the course of 8 h of white light irradiation, ≈ 50% of the degradation in water was observed (Figures S20 and S21, Supporting Information), indicating that ambient white light can cause degradation of the microstructure in water. Nevertheless, the white light-induced degradation is significantly slower compared to the specific blue-light LED set up where complete degradation was achieved after a shorter time of exposure. In a control experiment, the microstructures were submerged in water and left in darkness for an extended period of time (up to 80 h). We observed a reduction of the maximum height of these microstructures of ca. 30%, however no further degradation occurred (Figures S18 and S19, Supporting Information). The initial reduction of the heights may therefore be attributed to the diffusion of the water-soluble fractions that were not completely integrated within the structure during photocrosslinking, and concomitant compaction of the microstructures due to the exchange of water and organic solvent.

To highlight the potential of our photodegradable resists in tailoring microstructures post-fabrication, we designed a multimaterial structure by co-writing a commercial nonphotodegradable resist with our system. We selected so-called boxing-ring structures, i.e., four pillars arranged in a square with bridges suspended in between them, as they constitute a simple but powerful way to show that our resist can support its
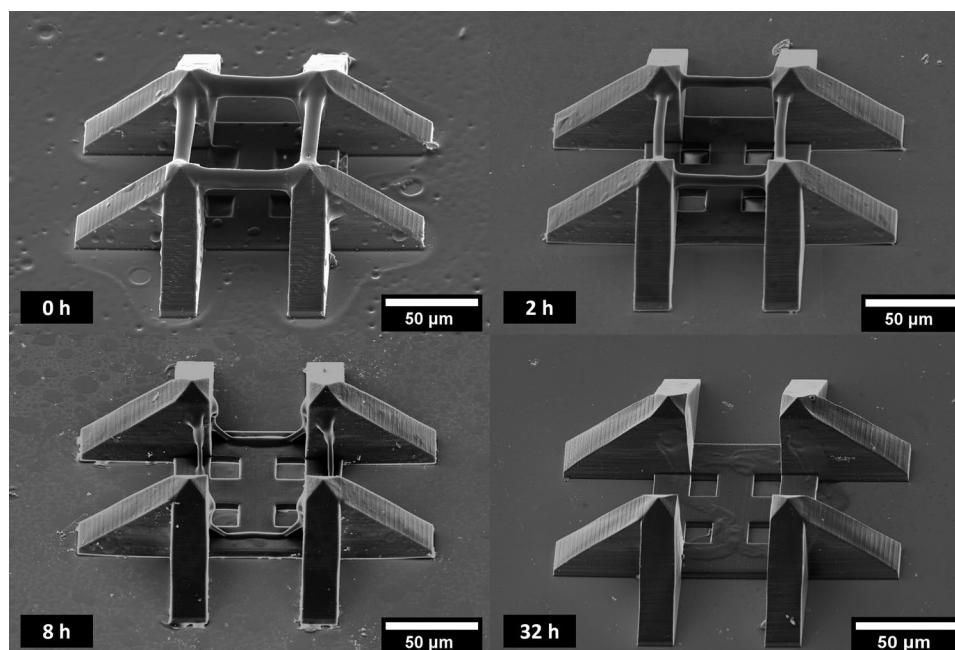
**ADVANCED
SCIENCE NEWS**

www.advancedsciencenews.com

**ADVANCED
MATERIALS**

www.advmat.de

Figure 5. SEM images of the degradation of boxing-ring microstructures in water under irradiation with a 10 W LED (λ_{max} = 415 nm). The frames were constructed from IP-S using a laser power of 16 mW and a scan speed of 3000 µm s^{-1}. The bridges were constructed from our photodegradable resist using a laser power of 14 mW and a scan speed of 200 µm s^{-1}.

own weight and retains its functionality in 3D structures.[13,30] The boxing rings are constructed following a two-step procedure (refer to Figure 1): First, the frames are printed from a commercial, non-adaptive resist (IP-S). Second, after a washing step, the bridges are printed in between the frames using our visible-light-degradable resist. Subsequently, the degradation of the boxing rings was induced using a 10 W λ_{max} = 415 nm LED in both pure water and a 1:1 mixture of water and acetonitrile. The degradation was followed by both light microscopy (Figure S25, Supporting Information) and SEM (**Figure 5**). After 2 h, the average thickness of the bridges decreased substantially (Figure S26, Supporting Information) by ca. 40%, from 9.1 to 5.4 µm. The photodegradation was accompanied by the bleaching of the bimane component within the microstructure, i.e., loss of yellow color, as seen from in the light microscopy images. After 8 h, the thickness of the bridges has decreased further, and they have started to collapse. Finally, after 32 h, the bridges have degraded completely, with only the frame consisting of commercial resist remaining.

3. Conclusion

We pioneer a resist system which can be degraded by visible light in aqueous environment. The time dependence of the degradation process has been carefully analyzed using AFM, revealing that water is an excellent solvent for the degradation to proceed. We further demonstrate the utility of our resist formulation for the fabrication of more complex 3D microstructures, where the microstructures are able to hold their own weight, while retaining their degradability. The current limiting factor of our system is the larger scale preparation of the photodegradable

bimane linker for the potential commercialization of the resist formulation. Nevertheless, we submit that our resist system, able to be degraded under such benign conditions—using visible light in water—may have broad applications in biological settings, including in single cell studies and biotherapeutics.

Supporting Information

Supporting Information is available from the Wiley Online Library or from the author.

Conflict of Interest

The authors declare no conflict of interest.

Data Availability Statement

The data that support the findings of this study are available from the corresponding author upon reasonable request.

Keywords

direct laser writing, microprinting, visible light degradation

[1] K.-S. Lee, R. H. Kim, D.-Y. Yang, S. H. Park, *Prog. Polym. Sci.* **2008**, *33*, 631.

[2] S. Maruo, O. Nakamura, S. Kawata, *Opt. Lett.* **1997**, *22*, 132.

[3] W. Xiong, L. Liu, L. J. Jiang, Y. S. Zhou, D. W. Li, L. Jiang, J.-F. Silvain, Y. F. Lu, *Adv. Mater.* **2016**, *28*, 2002.

[4] B.-B. Xu, Y.-L. Zhang, H. Xia, W.-F. Dong, H. Ding, H.-B. Sun, *Lab Chip* **2013**, *13*, 1677.

[5] A. K. Nguyen, R. J. Narayan, *Mater. Today* **2017**, *20*, 314.

[6] M. Hippler, E. D. Lemma, S. Bertels, E. Blasco, C. Barner-Kowollik, M. Wegener, M. Bastmeyer, *Adv. Mater.* **2019**, *31*, 1808110.

[7] C. Barner-Kowollik, M. Bastmeyer, E. Blasco, G. Delaittre, P. Müller, B. Richter, M. Wegener, *Angew. Chem., Int. Ed.* **2017**, *56*, 15828.

[8] S. C. Ligon, R. Liska, J. Stampfl, M. Gurr, R. Mülhaupt, *Chem. Rev.* **2017**, *117*, 10212.

[9] V. X. Truong, K. Ehrmann, M. Seifermann, P. A. Levkin, C. Barner-Kowollik, *Chem. Eur. J.* **2022**, *28*, e202104466.

[10] P. Mueller, M. M. Zieger, B. Richter, A. S. Quick, J. Fischer, J. B. Mueller, L. Zhou, G. U. Nienhaus, M. Bastmeyer, C. Barner-Kowollik, M. Wegener, *ACS Nano* **2017**, *11*, 6396.

[11] D. Gräfe, A. Wickberg, M. M. Zieger, M. Wegener, E. Blasco, C. Barner-Kowollik, *Nat. Commun.* **2018**, *9*, 2788.

[12] M. M. Zieger, P. Müller, E. Blasco, C. Petit, V. Hahn, L. Michalek, H. Mutlu, M. Wegener, C. Barner-Kowollik, *Adv. Funct. Mater.* **2018**, *28*, 1801405.

[13] D. Gräfe, M. Gernhardt, J. Ren, E. Blasco, M. Wegener, M. A. Woodruff, C. Barner-Kowollik, *Adv. Funct. Mater.* **2021**, *31*, 2006998.

[14] R. Batchelor, T. Messer, M. Hippler, M. Wegener, C. Barner-Kowollik, E. Blasco, *Adv. Mater.* **2019**, *31*, 1904085.

[15] C. Cardenas-Daw, A. Kroeger, W. Schaertl, P. Froimowicz, K. Landfester, *Macromol. Chem. Phys.* **2012**, *213*, 144.

[16] V. X. Truong, F. Li, J. S. Forsythe, *ACS Appl. Mater. Interfaces* **2017**, *9*, 32441.

[17] M. J. Kade, D. J. Burke, C. J. Hawker, *J. Polym. Sci., Part A: Polym. Chem.* **2010**, *48*, 743.

[18] A. Chaudhuri, Y. Venkatesh, K. K. Behara, N. D. P. Singh, *Org. Lett.* **2017**, *19*, 1598.

[19] J. L. Pelloth, P. A. Tran, A. Walther, A. S. Goldmann, H. Frisch, V. X. Truong, C. Barner-Kowollik, *Adv. Mater.* **2021**, *33*, 2102184.

[20] V. X. Truong, F. Li, J. S. Forsythe, *Biomacromolecules* **2018**, *19*, 4277.

[21] M. Carlotti, O. Tricinci, V. Mattoli, *Adv. Mater. Technol.* **2022**, *33*, 2101590.

[22] L. J. Jiang, Y. S. Zhou, W. Xiong, Y. Gao, X. Huang, L. Jiang, T. Baldacchini, J.-F. Silvain, Y. F. Lu, *Opt. Lett.* **2014**, *39*, 3034.

[23] J. Bauer, A. Guell Izard, Y. Zhang, T. Baldacchini, L. Valdevit, *Adv. Mater. Technol.* **2019**, *4*, 1900146.

[24] X.-Z. Dong, Z.-S. Zhao, X.-M. Duan, *Appl. Phys. Lett.* **2008**, *92*, 091113.

[25] Y. Li, F. Qi, H. Yang, Q. Gong, X. Dong, X. Duan, *Nanotechnology* **2008**, *19*, 055303.

[26] S. Maruo, T. Hasegawa, N. Yoshimura, *Opt. Express* **2009**, *17*, 20945.

[27] A. Bauhofer Anton, S. Krödel, J. Rys, R. Bilal Osama, A. Constantinescu, C. Daraio, *Adv. Mater.* **2017**, *29*, 1703024.

[28] Y. Gan, *Surf. Sci. Rep.* **2009**, *64*, 99.

[29] K. Nishi, K. Fujii, Y. Katsumoto, T. Sakai, M. Shibayama, *Macromolecules* **2014**, *47*, 3274.

[30] M. Gernhardt, H. Frisch, A. Welle, R. Jones, M. Wegener, E. Blasco, C. Barner-Kowollik, *J. Mater. Chem. C* **2020**, *8*, 10993.